

# Microgrid Optimal Energy Scheduling Considering Neural Network based Battery Degradation

Cunzhi Zhao, *Student Member, IEEE* and Xingpeng Li, *Senior Member, IEEE*

**Abstract**— Battery energy storage system (BESS) can effectively mitigate the uncertainty of variable renewable generation. Degradation is unpreventable and hard to model and predict for batteries such as the most popular Lithium-ion battery (LiB). In this paper, we propose a data driven method to predict the battery degradation per a given scheduled battery operational profile. Particularly, a neural network based battery degradation (NNBD) model is proposed to quantify the battery degradation with inputs of major battery degradation factors. When incorporating the proposed NNBD model into microgrid day-ahead scheduling (MDS), we can establish a battery degradation based MDS (BDMDS) model that can consider the equivalent battery degradation cost precisely with the proposed cycle based battery usage processing (CBUP) method for the NNBD model. Since the proposed NNBD model is highly non-linear and non-convex, BDMDS would be very hard to solve. To address this issue, a neural network and optimization decoupled heuristic (NNODH) algorithm is proposed in this paper to effectively solve this neural network embedded optimization problem. Simulation results demonstrate that the proposed NNODH algorithm is able to obtain the optimal solution with lowest total cost including normal operation cost and battery degradation cost.

**Index Terms**— Battery degradation, Battery energy storage system, Energy management system, Machine learning, Microgrid day-ahead scheduling, Neural network, Optimization.

## NOMENCLATURE

*Sets:*

$S_T$	Set of time intervals.
$S_G$	Set of controllable micro generators.
$S_S$	Set of energy storage systems.
$S_{WT}$	Set of wind turbines.
$S_{PV}$	Set of PV systems.

*Parameters:*

$c_{Gi}$	Linear cost for controllable unit $i$ .
$c_{Gi}^{NL}$	No load cost for controllable unit $i$ .
$c_{Gi}^{SU}$	Start-up cost for controllable unit $i$ .
$\Delta T$	Length of a single dispatch interval.
$R_{prcent}$	Percentage of the backup power to the total power.
$E_{Si}^{Max}$	Maximum energy capacity of ESS $i$ .
$E_{Si}^{min}$	Minimum energy capacity of ESS $i$ .
$U_{Buy}^t$	Status of buying power from main grid in time interval $t$ .
$U_{Sell}^t$	Status of selling power to main grid status in time $t$ .
$c_{Buy}^t$	Wholesale electricity purchase price in time interval $t$ .
$c_{Sell}^t$	Wholesale electricity sell price in time interval $t$ .
$P_{Gi}^{Max}$	Maximum capacity of generator $i$ .

Cunzhi Zhao and Xingpeng Li are with the Department of Electrical and Computer Engineering, University of Houston, Houston, TX, 77204, USA (e-mail: czhao20@uh.edu; Xingpeng.Li@asu.edu).

$P_{Gi}^{Min}$	Minimum capacity of generator $i$ .
$P_{Gi}^t$	Output of generator $i$ in time interval $t$ .
$U_{Char}^{t,i}$	Charging status of energy storage system $i$ in time interval $t$ . It is 1 if charging status; otherwise 0.
$U_{Disc}^{t,i}$	Discharging status of energy storage system $i$ in time interval $t$ . It is 1 if discharging status; otherwise 0.
$U_G^{ti}$	Status of generator $i$ in time interval $t$ . It is 1 if on status; otherwise 0.
$V_G^{ti}$	Startup indicator of Status of generator $i$ in time interval $t$ . It is 1 if unit $i$ starts up; otherwise 0.
$P_{Buy}^t$	Amount of power purchased from main grid power in time interval $t$ .
$P_{Sell}^t$	Amount of power sold to main grid power in time interval $t$ .
$P_L^t$	Demand in the microgrid in time interval $t$ .
$P_{Disc}^{t,i}$	Discharging power of energy storage system $i$ at time $t$ .
$P_{Char}^{t,i}$	Charging power of energy storage system $i$ at time $t$ .
$P_{Grid}^{Max}$	Maximum thermal limit of tie-line between main grid and microgrid.
$P_{Gi}^{Ramp}$	Ramping limit of diesel generator $i$ .
$P_{Si}^{Max}$	Maximum charge/discharge power of BESS $i$ .
$P_{Si}^{Min}$	Minimum charge/discharge power of BESS $i$ .
$\eta_{Si}^{Disc}$	Discharge efficiency of BESS $i$ .
$\eta_{Si}^{Char}$	Charge efficiency of BESS $i$ .

## I. INTRODUCTION

Renewable energy sources (RES) will play an important role in future microgrid due to the 3-D (decentralization, decarbonation, and digitalization) trend. The proportion of RES in power generation is growing significantly. However, the system stability is substantially weakened by the stochastic and intermittent generation of high penetration RES. Battery energy storage system (BESS) is an effective flexible solution for addressing the uncertainty of variable RES induced system [1]. Thus, much more BESSs will be available in bulk power systems and small-scale microgrids in near future.

The characteristic of rechargeable battery makes it degrade during cycling. This degradation can be accelerated by extreme fast charging or discharging cycles, extreme low or high ambient temperature and over charging or over discharging. The internal states of battery remain difficult to estimate while the battery is taking a more important role as BESS in power energy systems [2]. Therefore, the battery degradation is quite hard to predict. The working principle of a BESS is similar to a voltage source in series with impedances. However, the operating conditions and environments are various for BESS in microgrids, as well as in bulk power systems. Thus, the BESS model cannot be simply treated as a voltage-source based

model [3]. Li-ion battery (LiB) has been widely used as energy storage due to its high energy density and low memory effect nature. LiB degrades mainly because of the loss of Li-ions, the loss of electrolyte and the increase of internal resistance. During battery cycling, the influential factors that cause the degradation include the battery operating ambient temperature, charging/discharging rate, state of charge (SOC), state of health (SOH), and depth of discharge (DOD) [4]-[6].

Previous studies have developed some energy management strategies of BESS-integrated microgrids. In [7]-[14], it has been proved that the BESS can be seamlessly integrated into microgrid especially for those microgrids with high penetration renewable energy sources. However, they did not consider the effect of battery degradation.

Some simple models of battery degradation are proposed in the literature. In [15], DOD is used to calculate the remaining useful cycles. The battery degradation is estimated based on the remaining useful battery cycle and the actual capacity. The only variable considered in [15] is the DOD and they assume the degradation process to be linear throughout the battery life which is not reasonable. Pascali in [16] adopts the Butler-Volmer equation for battery degradation model to illustrate the diffusion of the solvent reactants. However, the degradation data are based on the experiment for different discharge currents and SOC values, which are not sufficient as they omit other important factors contributing to battery degradation. As mentioned in [17]-[20], the linear assumption of battery degradation may simplify the problem and reduce the computational difficulty, but the degradation value may not be accurately predicted.

Saldana's paper [21] proposed a battery degradation matrix reference for electric vehicle (EV). However, it is impractical to consider this model in the microgrid day-ahead scheduling (MDS) problem. The electric vehicle has been researched and conducted in the V2G system in [22]-[24] due to the similarity between EV and BESS. However, an important EV battery degradation factor, the charge/discharge rate, is neglected in those papers. A data driven degradation model is presented in [25]. A quadratic equation is formed based on the collected data; however, the data are collected only under different profiles of DOD and SOC. For all the aforementioned battery degradation models, they ignore several critical degradation factors, which limits accuracy of the battery degradation prediction; in addition, none of them provides a comprehensive model to capture all critical degradation factors; moreover, some of the degradation models are too complex to be incorporated into MDS.

[26]-[28] presents some advanced methodology to predict the lifetime of the battery cell and then the degradation can be averaged for each cycle. However, those methodologies are designed especially for the battery aging tests in which the battery's cycle is set as a fixed charge or discharge rate. In other words, the battery degradation or remaining cycle prediction is based on the fixed charging or discharging cycles in those methodologies. Therefore, those advanced methodologies cannot reflect the degradation prediction for usage-based BESS due to the dynamic and various charge or discharge rate at different time interval in power system applications.

To address the above-mentioned gaps, a fully connected neural network (NN) is proposed to train a battery degradation

model, and a cycle based battery usage processing (CBUP) method is developed for the BESS scheduling to accurately predict the battery degradation with the proposed NN model. The input of the NN model is a vector of five features including ambient temperature, charging/discharging rate, SOC, DOD and SOH. This neural network based battery degradation (NNBD) model contains non-linear activation functions in the hidden layers, which makes it complex. When incorporating the proposed NNBD model into MDS, we can establish a battery degradation based MDS (BDMDS) model that can consider the equivalent battery degradation cost.

The BESS scheduling in MDS does not always operate in a fixed charging or discharging cycle. Therefore, the CBUP method is designed to fill the research gap between the fixed-cycle based NNBD model and the dynamic BESS operation in MDS. However, such a complex neural network embedded optimization problem would be hard to solve directly. To address this issue, a neural network and optimization decoupled heuristic (NNODH) algorithm is proposed in this paper to effectively solve the BDMDS problem. The proposed NNODH algorithm iteratively solves the transformed BDMDS problem that is decoupled to the battery degradation calculation and MDS optimization problems. BESS operation constraints with tighter bounds will be generated in each iteration to limit the usage of BESS which can reduce the battery degradation and the relevant cost in the next iteration. However, the microgrid's operation cost will increase if the BESS usage is limited. The goal of the proposed NNODH algorithm is to find the lowest value for the sum of battery degradation cost and microgrid operation cost. It can also record the total cost for each iteration and locate the vertex point which is also the optimal solution for the BDMDS problem. Three benchmark models are also developed to test and compare the performance of the proposed NNODH algorithm. The main contributions of this paper are summarized as follows:

- A set of battery cycle generators is designed to simulate battery degradation under different battery operational profiles. The key features (ambient temperature, charge/discharge rate, SOC level, DOD and updated battery energy capacity) that affect battery degradation are collected for each cycle.
- A neural network based battery degradation model with the above five input features is proposed in this paper and it is able to accurately predict the degradation respect to the current maximum battery energy capacity.
- A CBUP method is proposed to process the BESS profile to correctly incorporate the proposed NNBD model into MDS, addressing the inconsistency between the fixed-cycle based NNBD model and BESS scheduling.
- A BDMDS model is proposed to capture the effect of battery degradation by incorporating the proposed NNBD model into microgrid energy management.
- An NNODH algorithm is proposed to efficiently solve the BDMDS model that is hard to solve directly. Four battery usage-limiting MDS models, referred to as conserved MDS (CMDS), are developed and used by the NNODH method. The optimal scheduling obtained with NNODH leads to the lowest total cost including the battery degradation cost and microgrid operation cost.

- Validation of the performance for the proposed NNODH algorithm is conducted. Case studies prove that by limiting the battery operation that leads to lower degradation, the total cost can be reduced significantly.

The rest of the paper is organized as follows. Section II presents a traditional MDS model. Section III presents the neural network structure of the proposed battery degradation model and Section IV presents the proposed microgrid energy management strategies with the BESS degradation model. Section V discusses the microgrid testbed, simulation results and sensitivity analysis. Section VI concludes the paper.

## II. TRADITIONAL MICROGRID DAY-AHEAD SCHEDULING

A traditional MDS model is established as a basic model to gauge the proposed BDMDS model. This traditional MDS model consists of (1)-(15) as described below and it does not consider battery degradation.

The objective of this traditional MDS model is to minimize the total cost of the microgrid operations as illustrated in (1). The power balance equation involving controllable generators, renewable energy sources, power exchange with the main grid, BESS output and the load is shown in (2). Constraint (3) enforces the power limits of the controllable units such as diesel generators. The ramping up and down limits are enforced by (4) and (5). Equation (6) ensures the status of power exchange between microgrid and main grid to be either purchasing or selling or stay idle. The thermal limit of the tie-line is enforced by constraints (7)-(8). Equation (9) restricts the BESS to be either in charging mode or in discharging mode or stay idle. Constraints (10)-(11) limit the charging/discharging power of BESS. As shown in (12), the SOC level of BESS can be calculated based on current energy stored in BESS. Equation (13) calculates the energy stored in the BESS for each time interval. The ending SOC level of BESS is forced to be equal to the initial SOC value (14). Constraint (15) ensures the microgrid to have sufficient backup power to address outage events.

Objective:

$$f^{MG} = \sum \sum (P_{Gi}^t c_{Gi} + U_{Gi}^t c_{Gi}^{NL} + V_{Gi}^t c_{Gi}^{SU}) + P_{Buy}^t c_{Buy}^t - P_{Sell}^t c_{Sell}^t, \forall i, t \quad (1)$$

Constraints are as follows:

$$\begin{aligned} P_{Buy}^t + \sum_{i \in S_G} P_{Gi}^t + \sum_{i \in S_{WT}} P_{WTi}^t + \sum_{i \in S_{PV}} P_{PVi}^t \\ + \sum_{i \in S_S} P_{Disc}^{t,i} \\ = P_{Sell}^t + \sum_{i \in S_L} P_{Li}^t \\ + \sum_{i \in S_S} P_{Char}^{t,i} \end{aligned} \quad (2)$$

$$P_{Gi}^{Min} \leq P_{Gi}^t \leq P_{Gi}^{Max}, \forall i, t \quad (3)$$

$$P_{Gi}^{t+1} - P_{Gi}^t \leq \Delta T \cdot P_{Gi}^{Ramp}, \forall i, t \quad (4)$$

$$P_{Gi}^t - P_{Gi}^{t+1} \leq \Delta T \cdot P_{Gi}^{Ramp}, \forall i, t \quad (5)$$

$$U_{Buy}^t + U_{Sell}^t \leq 1, \forall t \quad (6)$$

$$0 \leq P_{Buy}^t \leq U_{Buy}^t \cdot P_{Grid}^{Max}, \forall t \quad (7)$$

$$0 \leq P_{Sell}^t \leq U_{Sell}^t \cdot P_{Grid}^{Max}, \forall t \quad (8)$$

$$U_{Disc}^{t,i} + U_{Char}^{t,i} \leq 1, \forall i, t \quad (9)$$

$$U_{Char}^{t,i} \cdot P_{Si}^{Min} \leq P_{Char}^{t,i} \leq U_{Char}^{t,i} \cdot P_{Si}^{Max}, \forall i, t \quad (10)$$

$$U_{Disc}^{t,i} \cdot P_{Si}^{Min} \leq P_{Disc}^{t,i} \leq U_{Disc}^{t,i} \cdot P_{Si}^{Max}, \forall i, t \quad (11)$$

$$SOC_{Si}^t = E_{Si}^t / E_{Si}^{Max}, \forall i, t \quad (12)$$

$$E_{Si}^t - E_{Si}^{t-1} + \Delta T \cdot (P_{Disc}^{t-1,i} / \eta_{Si}^{Disc} - P_{Char}^{t-1,i} \eta_{Si}^{Char}) = 0, \forall i, t \quad (13)$$

$$E_{Si}^{t=24} = E_{Si}^{Initial}, \forall i \quad (14)$$

$$\begin{aligned} P_{Grid}^{Max} - P_{Buy}^t + P_{Sell}^t + \sum_{G \in S_G} (P_{Gi}^{Max} - P_{Gi}^t) \\ \geq R_{percent} \left( \sum_{i \in S_L} P_{Li}^t \right), \forall i, t \end{aligned} \quad (15)$$

## III. NEURAL NETWORK BASED BATTERY DEGRADATION MODELING

The traditional microgrid day-ahead scheduling model determines the optimal operational profiles for BESS, controllable generators and tie-line exchange power. However, the BESS in the traditional MDS model is considered to be ideal without any degradation and the equivalent cost of battery degradation is zero. This may substantially accelerate the aging and replacement of expensive BESS which may lead to economic loss in the long run. Besides, the BESS degradation needs to be accurately quantified for various battery daily operational profiles to obtain the truly optimal scheduling solutions. Thus, a deep learning method, particularly a deep neural network, is proposed in this section to accurately predict the BESS degradation.

### A. Input Data

The deep neural network is applied to learn and predict the battery degradation with several critical features. A battery model implemented in the MATLAB Simulink [29] is used to conduct the battery aging tests. This battery model can simulate various types and configurations of batteries, various conditions, and operating profiles. Built upon this battery model, a battery cycle generator is designed to simulate the charging and discharging cycles under preset charging/discharging rates. For each battery aging test, each cycle is simulated to discharge from a certain SOC to a certain lower SOC and then charge back to the starting SOC. The data collected from the battery aging tests include the ambient temperature, charging/discharging rate, SOC, DOD and reduced energy capacity level. The battery's energy capacity level for each cycle is also used to calculate each cycle's battery degradation value. Table I lists the numbers of battery aging tests that are simulated under different SOC and DOD. Each battery aging test represents a group of simulated battery profile under initial SOC and fixed DOD until the battery capacity degrades to 80% of the maximum rated capacity. This indicates each battery aging test may contain different numbers of cycles. It is common to consider the 80% of the rated capacity as the end of battery's life in battery aging test [30]. For instance, the "4" in Table I means there are four battery aging tests that are simulated at an initial SOC level of 100% with a DOD level of 10%. Moreover, each of these SOC&DOD combinations will be simulated under different ambient temperatures and charging/discharging rates. The charging/discharging rate is also referred as C rate. As shown in (16), C rate measures the speed at which a battery is fully charged or discharged.

$$C \text{ rate} = \frac{I_{\text{Battery}}}{E_0} \quad (16)$$

where  $I_{\text{Battery}}$  represents the charging/discharging current of the BESS and  $E_0$  denotes the rated capacity of BESS. For example, 2C means the battery will discharge the full capacity in 0.5 hour. This work conducted 945 different battery aging tests with different values of degradation factors.

TABLE I Numbers of battery aging tests under various SOC and DOD levels

DOD	Initial SOC					
	100%	80%	60%	50%	40%	20%
20%	4	5	17	23	22	23
30%	20	34	36	32	37	/
40%	36	41	41	40	44	/
50%	38	41	36	42	/	/
60%	37	37	37	/	/	/
70%	41	36	/	/	/	/
80%	39	35	/	/	/	/
90%	35	/	/	/	/	/
100%	36	/	/	/	/	/

### B. Data Pre-processing

The battery capacity level or SOH in percent at the end of each cycle is recorded from each simulation of battery aging test. Battery degradation per cycle is defined as the difference between the initial SOH and ending SOH for a given cycle. However, for some battery aging tests with low C rates and small DODs, the degradation for some cycles may be too less to measure and could even be zero. Also, some of the degradation data contain outlier points which may require some further process for a better training result. The battery degradation data are processed with different methods: (i) raw, (ii) smoothed method, and (iii) regressed method, as shown in Fig. 1. “Raw” represents the original data without any pre-processing and the associated training results can be used as a benchmark to gauge the effectiveness of the other two proposed data pre-processing methods. The smoothed method filters out the outliers of the raw data. Regressed method applies linear regression on the smoothed data. All three groups of input data are normalized to increase the training efficiency. The normalization used in [31] is applied in the data pre-processing and shown in (17):

$$\widehat{x}_k = \frac{x_k - E(x_k)}{\sqrt{Var(x_k)}} \quad (17)$$

where  $E(x_k)$  represents the expectation of  $x_k$  and  $Var(x_k)$  represents the variance of the  $x_k$ . The input data will be split into two parts, 80% as the training dataset and 20% as the validation dataset. At last, three groups of data will be fed into the NN separately to evaluate their performance.

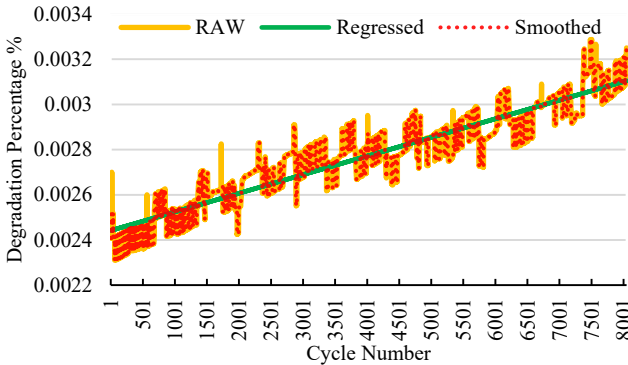


Fig. 1. Battery degradation data under different data processing methods.

### C. The Proposed NNBD Model

A fully connected neural network is constructed to model the battery degradation. Five aging factors (ambient temperature, C rate, SOC, DOD and SOH) form a five-element input vector for the neural network. Each input vector corresponds to a single output value which is the amount of battery degradation in percentage respect to the SOH level for the same cycle. A dynamic learning rate scheme is used in the training process to improve the training result. The learning rate will decrease automatically after a certain number of training epochs. The structure of the trained neural network is shown in Fig. 2 plotted by NN-SVG [32]. It has an input layer with 5 neurons, first hidden layer with 20 neurons, second hidden layer with 10 neurons and an output layer with 1 neuron. The activation function for the hidden layers is “relu” and “linear” for the output layer.

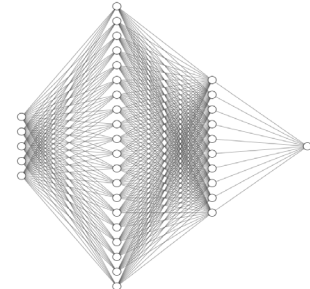


Fig. 2 Structure of the proposed neural network model for battery degradation.

Mini batch gradient descent strategy is applied to train the neural network. Different batch sizes are tested to achieve the best training results. As defined in (18), mean squared error (MSE) represents the average of the square of the difference between the actual and predicted values over all training data points. MSE is used as the criterion, a loss function, to train the neural network and measure the neural network quality.

$$MSE = \frac{1}{n} \sum_{i=1}^n (y_i - \tilde{y}_i)^2 \quad (18)$$

### D. Battery Degradation Calculation

From the BESS operation profile, the SOC level is required as the input of the proposed NNBD model. The absolute value of the difference in the SOC levels between time intervals  $t$  and  $t - 1$  will be the DOD level as shown in (19). C rate is calculated by (20). It is assumed that the battery SOH level is available for microgrid day ahead scheduling, which is practical. The input vector can be formed as shown in (21) and then be fed into the trained neural network to obtain the total battery degradation (BD) over the MDS time horizon in (22).

$$DOD_t = |SOC_t - SOC_{t-1}| \quad (19)$$

$$C_t^{\text{Rate}} = DOD_t / \Delta T \quad (20)$$

$$\bar{x}_t = (T, C, SOC, DOD, SOH) \quad (21)$$

$$BD = \sum_{t \in S_T} f^{NN}(\bar{x}_t) SOH \quad (22)$$

### E. Cycle Based Battery Usage Processing Method

The equation (22) for battery degradation calculation mentioned in the previous section covers all the time periods for the microgrid day ahead scheduling. However, the BESS is not scheduled in fixed cycles with constant charge/discharge rates in the same cycle per MDS, leading to inconsistency with the fixed-cycle based data that are used for training NNBD. Furthermore, the idle status is also considered in the (22) but it

is out sampled for the NNBD model. In other words, equation (22) considers each time interval as a BESS cycle and feeds the associated data directly into the NNBD model, which may not accurately predict the BESS degradation. Therefore, the proposed CBUP method is developed to address the inconsistency and accurately apply the proposed NNBD model in the MDS problem.

In the CBUP method, instead of considering each time interval as a cycle, the operating time intervals of BESS scheduling are combined and averaged into different cycles. For any continuous time intervals, if the operation status (charging or discharging) does not change, they will be aggregated as a single charging or discharging cycle. For the aggregated cycle, the charging or discharging power will be the average of the aggregated time periods. The SOC will be the initial SOC value of the first time period in the aggregated time periods and the DOD will be the absolute value of the SOC difference between the start time period and the end time period respectively. Thus, equation (22) is replaced by (23) while  $\bar{x}_c$  represents the input vector for the aggregated cycles and  $AC$  represents the set of feasible aggregated cycles.

$$BD = \sum_{c \in AC} f^{NN}(\bar{x}_c) SOH \quad (23)$$

#### F. Incorporating NNBD into Microgrid Scheduling

When considering battery degradation in microgrid day-ahead scheduling, the objective function needs to be updated by including the associated equivalent battery degradation cost. The updated objective function is as follows,

$$f = f^{MG} + f^{BESS} \quad (24)$$

where  $f^{MG}$  is defined in (1); and  $f^{BESS}$  denotes the battery degradation cost that can be estimated by the proposed NNBD model.  $f^{BESS}$  can be calculated as follows,

$$f^{BESS} = \frac{c_{BESS}^{Capital} - c_{BESS}^{SV}}{1 - SOH_{EOL}} BD \quad (25)$$

where  $c_{BESS}^{Capital}$  represents the capital investment cost of BESS;  $c_{BESS}^{SV}$  denotes the salvage value at the end of life;  $SOH_{EOL}$  represents state of health value that the BESS is considered as the end of life;  $BD$  represents the percentage battery degradation calculated by (23).

Thus, the proposed BDMDS model can be represented by (2)-(15), (19)-(21), and (23)-(25).

## IV. THE PROPOSED NNODH FOR MICROGRID SCHEDULING

The proposed battery degradation based microgrid day-ahead scheduling model, which is presented in the above section, would be very hard to solve directly since the proposed NNBD model that is highly non-linear and non-convex is now a part of the proposed BDMDS model. To address this issue, a novel method, NNODH, is proposed in this paper to decouple the complex BDMDS model and solve it in the following five steps in an iterative manner.

- Step A is to solve the microgrid day-ahead scheduling with additional constraints by limiting BESS usage that is generated from Step E. Note that in the first iteration, there is no extra limit on BESS usage.
- Step B obtains the scheduled BESS operating profile that is then processed with the proposed CBUP method.

- Step C estimates BESS degradation with the proposed NNBD model that is trained beforehand and calculates the associated equivalent battery degradation cost.
- Step D determines whether the solutions meet the designed stopping criteria: stop the iteration process and report the solution if yes; otherwise, go to Step E.
- Step E updates the boundaries that limit the BESS operations to reduce the degradation cost; and the associated constraints will be sent to Step A to be included in MDS for the next iteration.

This iterative procedure is illustrated in Fig. 3.

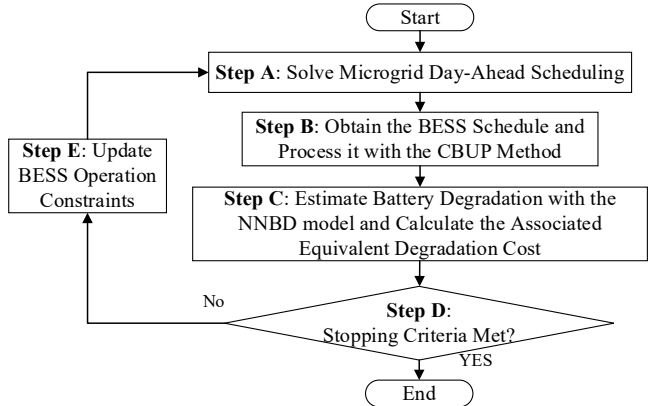


Fig. 3. Flowchart of the proposed NNODH method.

#### A. Microgrid Scheduling

The traditional microgrid day-ahead scheduling that is introduced in Section II is conducted to obtain an initial solution that does not consider the battery degradation. It is solved only once in the first iteration. When considering battery usage limiting constraints that will be presented in Section IV.D, Step A will solve the CMDS instead of the traditional MDS. To sum up, traditional MDS is solved in the first iteration while CMDS is solved in all subsequent iterations.

#### B. Operation Limits of BESS

The goal of Step E is to generate new constraints that can limit or change the battery output to reduce the total battery degradation. The generated constraints will further tighten the range that BESS can operate after each iteration. Three types of extra constraints are proposed to limit battery output. Constraint (26) named as battery consumption limit (BCL) is to reduce the sum of battery output power over 24 hours by forcing it to be less than the previous iteration. Constraint (27) only limits the sum of output power in three time intervals that have the highest battery charging or discharging power, named as precise battery consumption limit (PBCL). Constraints (28)-(29) are designed to limit the maximum charging/discharging power that is named as battery C rate limit (BRL). The proposed constraints will be generated and updated in each iteration by using the scheduled battery operational profile from previous iteration and the proposed battery operation restriction factor (BORF)  $\alpha$  which is a preset parameter. Note that the value of BORF can determine the limits in BCL, PBCL, and BRL for each iteration.

$$\sum_{t \in T} (P_{Char}^{t,i} + P_{Disc}^{t,i}) \leq (1 - \alpha) * P_{BatteryTotal}^{Previous\_SCUC} \quad (26)$$

$$\sum_{i \in Top 3} P_{Disc}^{t,i} + P_{Disc}^t \leq (1 - \alpha) * P_{BatteryTotal}^{Previous\_SCUC} \quad (27)$$

$$P_{Char}^{t,i} \leq P_{Si}^{Max} (1 - \alpha)^{iteration-1} \quad (28)$$

$$P_{Disc}^{t,i} \leq P_{Si}^{Max} (1 - \alpha)^{iteration-1} \quad (29)$$

Depending on which battery usage limiting constraint is used in CMDS, there are four variations of the proposed NNODH algorithm. They are all conducted to compare the performance of the proposed constraints. The proposed four variations are presented in Table II. The CMDS model in this table is solved instead of the traditional MDS model starting from the second iteration of the proposed NNODH algorithm.

TABLE II The proposed four NNODH strategies

Strategies	CMDS Model for Step A
NNODH-BCL	(1)-(15), (26)
NNODH-PBCL	(1)-(15), (27)
NNODH-BRL	(1)-(15), (28)-(29)
NNODH-ALL	(1)-(15), (26)-(29)

### C. Iterations and Stopping Criteria

Fig. 4 illustrates the iteration process of determining the optimal solution for BDMDS using the proposed NNODH algorithm. As is discussed in Section IV.A, the first iteration only considers the traditional microgrid day-ahead scheduling model that ignores the battery degradation. In Fig. 4, the red star denotes the global optimal solution for BDMDS that considers the proposed NNBD model; and the black star represents the solution for MDS/CMDS problem in the current iteration while the grey star denotes the solution for the MDS/CMDS problem in the previous iteration. The MDS/CMDS solutions are approximations to the global optimal solution for BDMDS; they are referred to as pseudo solutions (feasible but may not be global optimal) for BDMDS. Graph 1 in Fig. 4 represents the first iteration. The BESS usage limit constraints that are generated in each iteration will reduce the feasible region for the MDS/CMDS problem in the next iteration. Graphs 2-4 show the feasible region shrinks for each iteration and the black star (pseudo solution) is moving towards the red star (global optimal solution for BDMDS). Graph 5 shows the red star and black star overlap which indicates that the black star here is the optimal solution for the BDMDS problem. If the iteration continues, the feasible solution area of BDMDS will continue to reduce such that the optimal solution might be cut out. Practically, the pseudo solutions may not include the exact global optimal solution. Since the proposed NNODH algorithm is an iterative method, the BORF values in (26)-(29) would change over iterations and may result into different BDMDS solutions, among which the best solution should deviate slightly away from the global optimal solution. To ensure the best pseudo solution is close enough to the global solution with least total cost, small BORF is preferred. However, it may take more iterations for a smaller BORF to find the optimal solution.

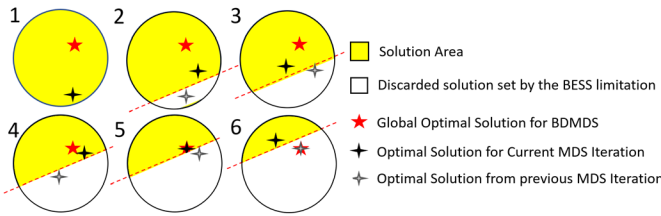


Fig. 4. Illustration of the proposed NNODH algorithm.

### D. Evaluation Metrics

Three metrics are designed to evaluate the performance of the proposed model: degradation cost reduction (DCR), total cost reduction (TCR) and operational cost increment (OCI). They are defined in (30), (31), and (32) respectively. The degradation cost reduction illustrates how much the battery degradation cost can be reduced as compared to the maximum value when battery degradation is not considered in traditional MDS. The TCR represents how much the total cost can be reduced by the proposed model while the OCI shows how much the operation cost would increase when considering the battery degradation model. Notations  $BDC^{Max}$ ,  $TC^{Max}$ ,  $OC^{Min}$  represent the maximum battery degradation cost, maximum total cost, and the minimum operation cost respectively. These metrics are obtained by solving the traditional MDS problem in the first iteration when battery degradation cost is not considered.

$$DCR = \frac{BDC^{Max} - BDC}{BDC^{Max}} * 100\% \quad (30)$$

$$TCR = \frac{TC^{Max} - TC}{TC^{Max}} * 100\% \quad (31)$$

$$OCI = \frac{OC - OC^{Min}}{OC^{Min}} * 100\% \quad (32)$$

A stopping criterion is proposed as part of the NNODH algorithm. It is used to terminate the iterations and then the best solution can be reported. The designed stopping criteria is defined as follows: for any past 10 iterations, if the  $TC^n - TC^{n-1}$  is less than 0 for the first five iterations but greater than 0 for the last five iterations, then the iteration will stop and the best solution with lowest total cost for BDMDS will be reported. Here,  $TC^n$  and  $TC^{n-1}$  denotes the total costs in  $n^{\text{th}}$  and  $(n-1)^{\text{th}}$  iterations respectively. The total cost here represents the lowest total cost rather than the lowest battery degradation cost. The optimal solution will be affected by the battery size as well as the unit price.

### E. Benchmark Models of MDS

Benchmark models are designed to evaluate and demonstrate the effectiveness and performance of the proposed NNODH algorithm. Three benchmark models are presented below and summarized in Table III:

1. Traditional MDS Model: The basic benchmark model is set with no BESS degradation cost and the MDS will maximize the usage of BESS to minimize the operation cost of the microgrid.
2. Cycle Limit Model: This model is widely adopted in the industry. It is designed to limit the charging and discharging cycles to decrease the degradation of the BESS. This model is formulated with the following constraints where the  $V_{Char/Disc}^{t,i}$  is a binary variable that represents the status change of charging or discharging operation.

$$V_{Char/Disc}^{t,i} \leq U_{Char/Disc}^{t,i} + U_{Char/Disc}^{t-1,i}, \forall i, t \quad (33)$$

$$V_{Char/Disc}^{t,i} \geq U_{Char/Disc}^{t,i} - U_{Char/Disc}^{t-1,i}, \forall i, t \quad (34)$$

$$V_{Char/Disc}^{t,i} \geq U_{Char/Disc}^{t-1,i} - U_{Char/Disc}^{t,i}, \forall i, t \quad (35)$$

$$V_{Char/Disc}^{t,i} \leq 2 - U_{Char/Disc}^{t,i} - U_{Char/Disc}^{t-1,i}, \forall i, t \quad (36)$$

$$V_{Char/Disc}^1 = 0 \quad (37)$$

$$\sum_t V_{Char/Disc}^{t,i} \leq 2 \quad (38)$$

3. Linear Battery Degradation Cost (BDC) Model: The third benchmark model is based on constant battery degradation cost parameters. It is assumed that the battery degradation cost is linear to the energy consumption of the BESS as shown in (39) where the  $c_{BESS}$  is a fixed rate that represents the battery degradation cost per unit usage of BESS.

$$f^{BESS} = c_{BESS} \sum_{t,i} P_{char/Disc}^{t,i} * \text{length}(t) \quad (39)$$

TABLE III Benchmarks models

MDS Models	Formulations
Traditional MDS	(1)-(15)
Cycle Limit	(1)-(15), (33-38)
Linear BDC	(1)-(15), (39)

## V. CASE STUDIES

### A. Microgrid Testbed

A typical grid-connected microgrid with renewable energy sources is created in this paper as a testbed to examine the proposed NNBD model, BDMDS model and NNODH algorithm. This testbed includes one 180kW diesel generator (DG), five 200kW wind turbines (WT), 300 residential houses that contains solar panel (5kW capacity per house), and a 300kWh lithium-ion based BESS with a charging/discharging efficiency of 90%. The load data representing 1000 residential houses. The ambient temperature and available solar power for a time period of 24 hours are obtained from the Pecan Street Dataport [33]. The wholesale electricity price is obtained from ECROT [34]. The price of the electricity sold to the main grid is set to 80% of the purchase price. Sensitivity analysis is conducted with different RES penetration levels and different BESS sizes. The computer with Intel® Xeon(R) W-2295 CPU @ 3.0 GHz, 256 GB of RAM, and Nvidia Quadro RTX 8000 (48GB GPU) was utilized to conduct the numerical simula-

tions including battery degradation model training and microgrid day-ahead resource scheduling. The microgrid resource scheduling problem studied in this work covers a total time horizon of 24 hours, which is solved using the Pyomo package [35] with the Gurobi solver [36].

### B. Training Results of NNBD

The training results of NNBD and hyperparameters are presented and analyzed in this section. Mini-batch technology is used for the NN training. The optimal batch size may vary for different input data. Different training batch sizes are tested to determine the optimal training batch-size and the test results are presented in Table IV. It can be observed that the batch size of 256 can achieve the highest accuracy while requiring less epochs to complete the training process. The validation accuracy can reach up to 94.5% while it only requires 50 epochs to reach a steady accuracy. The error tolerance is set to 15% when calculating prediction accuracy in Table IV and Table V. Larger or smaller batch size will either reduce the accuracy or increase the training epochs. We found that large batch size can help smooth the oscillation of the training accuracy curve. The training accuracies with batch sizes of 128 and 256 are almost equally the best. However, the training accuracy curve with a batch size of 256 is much smoother than the other one. Moreover, we observed that if the input data are shuffled, then the neural network cannot obtain good results. This may be due to the characteristic of the input data: the battery degradation data are time-series for each battery aging test. The results with different data pre-processing methods are compared in Table V. Note that the test results in Table V are obtained with the neural networks trained with the same batch-size of 256. The regressed data pre-processing method has the highest accuracy and efficiency. Based on the results from Table IV and Table V, the regressed method performs the best and is applied for all subsequent simulations.

Table IV Sensitivity test of batch-sizes

Batch-Size	16	32	64	128	256	512	1024	2048
Number of Epochs	20	20	85	110	50	50	75	75
Accuracy	40%	50%	90.5%	94.0%	94.5%	92.5%	88%	67%

Table V Training results with different data pre-processing methods

Data Pre-processing Methods	Accuracy	Number of Epochs
Raw	78%	150
Smoothed	82%	100
Regressed	94.5%	50

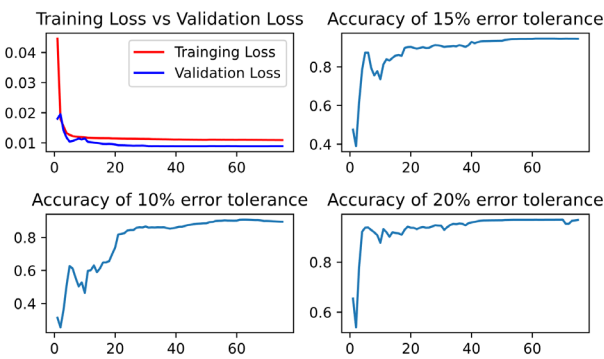


Fig. 5. Results of neural network training.

The best training results are shown in Fig. 5 that illustrates the training loss versus validation loss and the accuracy curves under different error thresholds. The accuracy is around 60% under a 5% error tolerance, 80% under a 10% error tolerance and 94.5% under a 15% error tolerance. The accuracy with 20% error tolerance is 95.5% which is only 1% higher than the 15% error tolerance. Thus, we choose 15% as the error tolerance level when calculating accuracy in all subsequent results. After 50 epochs, the training loss and the validation loss stop decreasing and the training accuracy becomes stable as well. The final training result stops at 65th epoch to avoid overfitting and oscillation.

### C. Results of NNODH algorithm

In this section, the BDMDS results obtained with the NNODH algorithm are presented. The load profile of the test bed is shown in Fig. 6. Table VI presents the results for different strategies of the proposed NNODH algorithm presented in Section IV. The BCL, PBCL, BRL and ALL CMDS models are implemented and tested separately. The combination of all

three types of constraints as the added constraints to MDS in the next iteration, marked as ALL in Table VI, is tested as well. In Table VI, for all the proposed models, the initial iteration does not have any limits of the BESS operation. This also leads to the solution of the first iteration having the highest battery degradation cost. Similarly, the maximum total cost for different models is the same. For DCR, the ALL option has the best performance among all strategies, and it decreases the battery degradation cost by 79.27%. BCL performs the best in terms of total cost reduction. The increased operation cost is similar between BCL and PBCL, which is less than BRL and ALL. Overall, we prefer the BCL due to its best performance to decrease the total cost and the fast solving time.

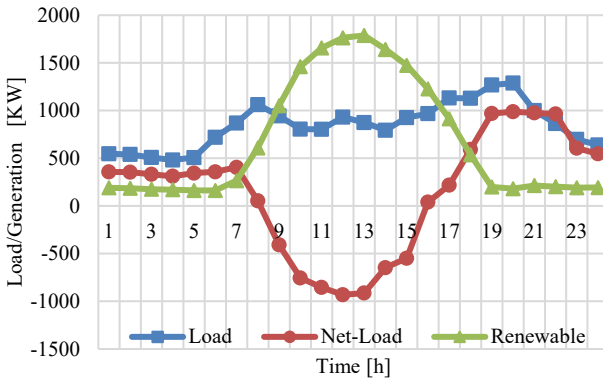


Fig. 6. Load profile of the microgrid testbed.

Table VI Results for proposed strategies

NNODH	BCL	PBCL	BRL	ALL
Total Cost (\$)	494.36	503.49	502.50	500.32
Degradation Cost (\$)	10.74	19.50	11.99	10.39
TCR	5.82%	4.08%	4.27%	4.69%
DCR	78.57%	60.23%	76.08%	79.27%
OCI	1.83%	1.81%	3.20%	3.09%
Solving time (s)	8.68	12.82	10.00	8.48
Iteration Numbers	37	56	46	37

Fig. 7 shows the results for NNODH-BCL including the degradation cost, operation cost, battery degradation in percent, and total cost. These results are based on the battery unit price of 400 \$/kWh and the value of BORF is set to 0.03. From Fig. 7, we can observe that the valley of the total cost curve is at the 37<sup>th</sup> iteration with \$494.36 including the equivalent battery degradation cost of \$10.74 and the microgrid operation cost of \$483.62. The total cost is reduced by 5.82% compared to the traditional MDS model that does not consider the battery degradation cost, which proves that the proposed NNODH algorithm can reduce the total cost significantly. Note that the results shown in Fig. 7 did not implement the stopping criteria to show how the system behaves when the battery's usage is further limited until idle. If not, the iteration will stop at the 42<sup>nd</sup> iteration since the minimum total cost can be found at the 37<sup>th</sup> iteration. After the 37<sup>th</sup> iteration, we can observe that even though the battery degradation cost keeps decreasing, the total cost starts to increase due to the increased slope of the operation cost.

The scheduled BESS operation for different models are shown in Fig. 8. Positive output means the BESS is in discharging mode and negative power means it is in charging mode. The scheduled BESS operations for the Traditional MDS model, Cycle Limit model, Linear BDC model and the

proposed BDMDS model are all shown in Fig. 8. It can be observed for the traditional MDS without the consideration of battery degradation, the BESS operates at a wider output range from -150 kW to 150 kW in seven different time intervals. When the degradation cost is considered, the BESS is scheduled to charge and discharge in a narrow range and in less active time intervals. The BESS operation patterns for different models match in most of the time intervals, which proves the effectiveness of those four models. For the proposed BDMDS, after applying the NNODH algorithm to solve it, the BESS operates only in three different time intervals. Total exchanged energy is limited to reduce the battery degradation which meets the designed purpose of BCL. The total usage of BESS for Traditional MDS model is 920 kWh while it is 325 kWh for BDMDS, 601 kWh for Cycle Limit model and 473 kWh for Linear BDC model.

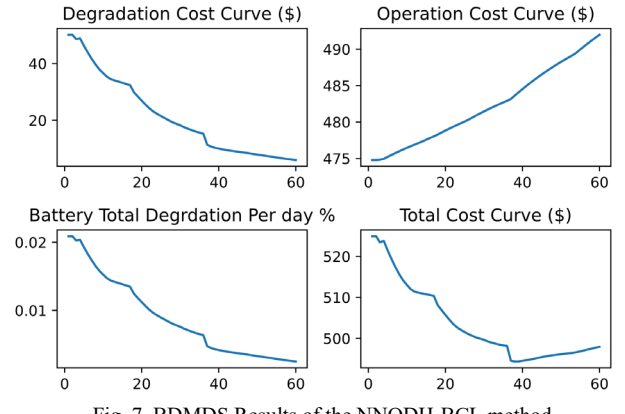


Fig. 7. BDMDS Results of the NNODH-BCL method.

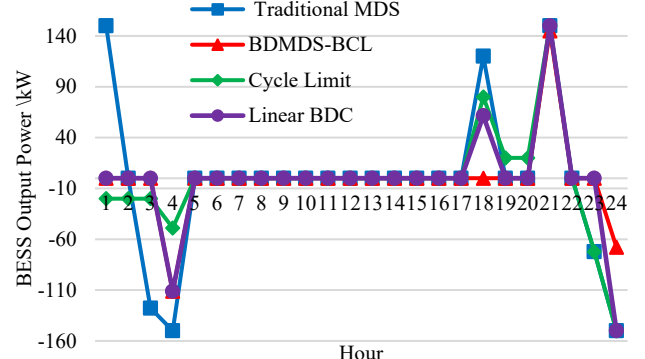


Fig. 8. BESS scheduled operations comparison.

Table VII presents the results of the CBUP method applied on the solutions obtained from BDMDS model and traditional MDS model. It can be clearly observed that the BD prediction is pretty close to the true BD in a small percent of error. Without the CBUP method, the error of BD prediction from NNBD model is significantly higher. Thus, the results proves the effectiveness of the proposed CBUP method. From Table VIII, we can observe that the proposed BDMDS model has the lowest daily degradation and the lowest annual degradation cost among all the models. Moreover, the BDMDS model is outstanding in annual cost saving. Also, if we consider the load profile is the same for each day, then the proposed BDMDS model can significant extend the lifetime of the BESS than all the benchmark models. Note that the expect end of life is set to 70% SOH.

Table IX shows the results of the sensitivity tests with different BORF values. The results show that larger BORF can achieve the lowest total cost in less iterations and less solving time. As a tradeoff, the optimal total cost of larger BORF will be slightly higher. Smaller BORF will lead to a smaller area cut from the feasible solution area in each iteration, which requires more iterations to converge to the optimal solution. However, the optimal solutions for the different BORFs do not have a significant difference. Thus, a higher value of BORF such as 0.05 is preferred due to the high computing efficiency.

Table VII Battery degradation prediction with different methods

Model	True BD	Without CBUP		With CBUP	
		Degradation	Error	Degradation	Error
BDMDS	0.00468%	0.037%	690%	0.0044%	5.9%
MDS	0.0108%	0.066%	511%	0.0120%	9.7%

Table VIII Model comparison

Model	Daily BESS Degradation	Annual Degradation Cost (\$)	Annual Cost Saving (\$)	Expect Lifetime (years)
MDS	0.02%	18,301.1	0	4.1
Cycle Limit	0.012%	12,540.8	6,205	6.8
Linear BDC	0.01%	8,832.5	6,935	8.2
BDMDS	0.0045%	3,920.1	11,151	18.3

Table IX Results of sensitivity analysis with different BORF values

BORF	Number of Iterations	Optimal Total Cost (\$)	Time (s)
0.01	113	494.35	25.21
0.02	57	494.35	12.51
0.03	38	494.36	8.42
0.05	22	494.36	5.20
0.1	11	494.38	2.85
0.2	5	494.40	1.41

#### D. Sensitivity Analysis of RES Penetration Levels

Table X presents the TCR and OCI results under different RES penetration levels for the microgrid. The penetration level is defined as the ratio of the average renewable generation to the average load for a typical day. The proposed microgrid testbed is set to an 80% RES penetration level. From Table X, we can observe that with the increase of RES penetration level, the value of TCR will increase and the value of OCI will decrease. This is because that in a system with higher RES penetration, BESS is needed more frequently to mitigate the uncertainty resulted by the RES generation, which leads to a higher battery degradation.

Table X Results of different RES penetration levels

	RES Penetration Level			
	20%	40%	60%	80%
TCR	1.60%	2.1%	3.12%	5.82%
OCI	0.47%	0.63%	0.94%	1.83%

#### E. Sensitivity Analysis of BESS Unit Prices and Sizes

In this section, the sensitivity analysis on different BESS unit prices and sizes is conducted. Fig. 9 shows that the total cost reduction in percentage. It can be clearly observed that for the same size of BESS, higher unit price corresponds to a higher total cost reduction in percent. For the same unit price of BESS, higher BESS size is tend to a lower TCR. Table XI shows that for the same unit price except \$200/kWh, higher BESS size has a lower DCR. This may be because that for the same battery output power, bigger battery size will likely have a lower C rate which is one of the main contributing factors of battery degradation. Also, for the same size BESS, higher unit

price lead to a higher DCR. Thus, we can conclude that the BESS price of per unit capacity is the major factor affecting how much the proposed model reduces the degradation cost. The BESS size is the major factor affecting how much the proposed model reduces the battery degradation. The result of the sensitivity analysis in this section may help determine the size of the BESS for microgrid planning. In the meanwhile, as the unit price of BESS keeps decreasing, the battery degradation cost will be lower and account for smaller percentage respect to the total cost in the future.

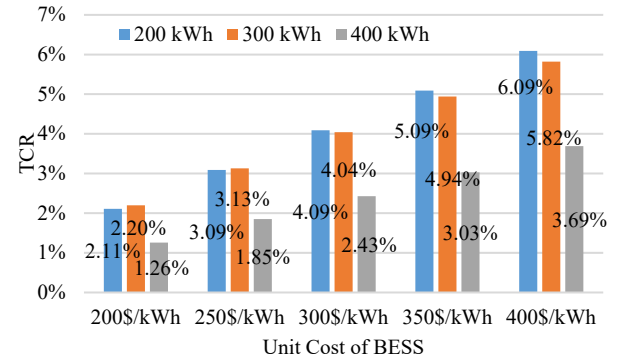


Fig. 9. Results of TCR sensitivity tests.

Table XI DCR of different BESS sizes and unit prices

Size (kWh)	Unit Price (\$/kWh)				
	200	250	300	350	400
200	75.15%	82.16%	82.96%	85.18%	88.58%
300	77.29%	77.29%	78.57%	78.57%	78.57%
400	52.95%	54.48%	54%	71.90%	72.68%

## VI. CONCLUSIONS

In this paper, a neural network based battery degradation model is proposed to predict the BESS degradation value for each scheduling period. A cycle based battery usage processing method is designed to accurately apply the proposed NNBD model with the MDS model. The NNODH algorithm is proposed to decouple the BDMDS problem that is hard to solve directly due to the highly non-linear characteristic of the proposed NNBD model. The proposed NNODH algorithm can solve the MDS optimization problem and calculate the battery degradation cost iteratively and effectively find the optimal solution with the lowest total cost. Four different types of constraints, BCL, PBCL, BRL and ALL are proposed to be integrated in the CMDS problem separately to limit the BESS usage to obtain a lower cost of battery degradation. An RES-enriched microgrid is used to evaluate the performance of the proposed BDMDS model and the proposed NNODH algorithm.

The test results demonstrate that the battery degradation can be accurately predicted by the proposed NNBD model with the adjusted inputs obtained by the proposed CBUP method. The proposed NNODH algorithm can obtain the optimal solution efficiently. The total cost can be reduced significantly with the proposed BDMDS model comparing to the traditional MDS model. The NNODH-BCL is proved to be the best among the proposed four NNODH strategies. Sensitivity tests demonstrate the performance of the proposed NNODH algorithm under different BESS sizes and unit prices. Overall, this work demonstrates the effectiveness of the proposed BDMDS model for reducing battery degradation cost and total cost, and

the capability of the proposed NNODH algorithm for efficiently solving BDMDS that is a deep neural network embedded optimization problem.

## REFERENCES

- [1] B. Li, T. Chen, X. Wang and G. Giannakis, "Real-Time Energy Management in Microgrids With Reduced Battery Capacity Requirements," *IEEE Trans. Smart Grid*, vol. 10, no. 2, pp. 1928–1938, Mar. 2019.
- [2] M. T. Lawder et al., "Battery Energy Storage System (BESS) and Battery Management System (BMS) for Grid-Scale Applications," in *Proceedings of the IEEE*, vol. 102, no. 6, pp. 1014-1030, June 2014.
- [3] X. Gong, R. Xiong and C. C. Mi, "Study of the Characteristics of Battery Packs in Electric Vehicles With Parallel-Connected Lithium-Ion Battery Cells," in *IEEE Transactions on Industry Applications*, vol. 51, no. 2, pp. 1872-1879, March-April 2015.
- [4] Z. Lyu, R. Gao, and L. Chen, "Li-Ion Battery State of Health Estimation and Remaining Useful Life Prediction Through a Model-Data-Fusion Method," *IEEE TRANSACTIONS ON POWER ELECTRONICS*, vol. 36, no. 6, pp. 6228–6240, June. 2021.
- [5] B. Xu, A. Oudalov, A. Ulbig, G. Andersson and D. Kirschen, "Modeling of lithium-ion battery degradation for cell life assessment," *2017 IEEE Power & Energy Society General Meeting*, 2017, pp. 1-1.
- [6] X. Han, L. Lu, Y. Zheng, X. Feng, Z. Li, J. Li, M. Ouyang, "A review of the key issues of the lithium ion battery degradation among the whole life cycle", in *eTransportation*, vol 1, Jul. 2019.
- [7] P. S. Kumar, R. P. S. Chandrasena, V. Ramu, G. N. Srinivas and K. V. S. M. Babu, "Energy Management System for Small Scale Hybrid Wind Solar Battery Based Microgrid," in *IEEE Access*, vol. 8, pp. 8336-8345, 2020.
- [8] A. Merabet, K. Tawfique Ahmed, H. Ibrahim, R. Beguenane and A. M. Y. M. Ghias, "Energy Management and Control System for Laboratory Scale Microgrid Based Wind-PV-Battery," in *IEEE Transactions on Sustainable Energy*, vol. 8, no. 1, pp. 145-154, Jan. 2017.
- [9] X. Xing, L. Xie, H. Meng, X. Guo, L. Yue and J. M. Guerrero, "Energy management strategy considering multi-time-scale operational modes of batteries for the grid-connected microgrids community," in *CSEE Journal of Power and Energy Systems*, vol. 6, no. 1, pp. 111-121, March 2020.
- [10] K. Thirugnanam, S. K. Kerk, C. Yuen, N. Liu and M. Zhang, "Energy Management for Renewable Microgrid in Reducing Diesel Generators Usage With Multiple Types of Battery," in *IEEE Transactions on Industrial Electronics*, vol. 65, no. 8, pp. 6772-6786, Aug. 2018.
- [11] Z. Miao, L. Xu, V. R. Disfani and L. Fan, "An SOC-Based Battery Management System for Microgrids," in *IEEE Transactions on Smart Grid*, vol. 5, no. 2, pp. 966-973, March 2014.
- [12] B. Li, T. Chen, X. Wang and G. B. Giannakis, "Real-Time Energy Management in Microgrids With Reduced Battery Capacity Requirements," in *IEEE Transactions on Smart Grid*, vol. 10, no. 2, pp. 1928-1938, March 2019.
- [13] C. Zhao and X. Li, "A Novel Real-Time Energy Management Strategy for Grid-Friendly Microgrid: Harnessing Internal Fluctuation Internally", *52nd North American Power Symposium*, (Virtually), Tempe, AZ, USA Apr. 2021.
- [14] C. Zhao and X. Li, "A Novel Real-Time Energy Management Strategy for Grid-Supporting Microgrid: Enabling Flexible Trading Power", *IEEE PES General Meeting*, (Virtually), Washington D.C., USA, Jul. 2021.
- [15] C. Ju, P. Wang, L. Goel and Y. Xu, "A Two-Layer Energy Management System for Microgrids With Hybrid Energy Storage Considering Degradation Costs," in *IEEE Transactions on Smart Grid*, vol. 9, no. 6, pp. 6047-6057, Nov. 2018.
- [16] L. De Pascali, F. Biral and S. Onori, "Aging-Aware Optimal Energy Management Control for a Parallel Hybrid Vehicle Based on Electrochemical-Degradation Dynamics," in *IEEE Transactions on Vehicular Technology*, vol. 69, no. 10, pp. 10868-10878, Oct. 2020.
- [17] J. Cao, D. Harrold, Z. Fan, T. Morstyn, D. Healey and K. Li, "Deep Reinforcement Learning-Based Energy Storage Arbitrage With Accurate Lithium-Ion Battery Degradation Model," in *IEEE Transactions on Smart Grid*, vol. 11, no. 5, pp. 4513-4521, Sept. 2020.
- [18] G. Abdelaal, M. I. Gilany, M. Elshahed, H. M. Sharaf and A. El'gharably, "Integration of Electric Vehicles in Home Energy Management Considering Urgent Charging and Battery Degradation," in *IEEE Access*, vol. 9, pp. 47713-47730, 2021.
- [19] K. Abdulla et al., "Optimal operation of energy storage systems considering forecasts and battery degradation," *2017 IEEE Power & Energy Society General Meeting*, 2017, pp. 1-1.
- [20] K. Antoniadou-Plytaria, D. Steen, L. A. Tuan, O. Carlson and M. A. Fotouhi Ghazvini, "Market-Based Energy Management Model of a Building Microgrid Considering Battery Degradation," in *IEEE Transactions on Smart Grid*, vol. 12, no. 2, pp. 1794-1804, March 2021.
- [21] G. Saldaña, J. I. S. Martín, I. Zamora, F. J. Asensio, O. Oñederra and M. González, "Empirical Electrical and Degradation Model for Electric Vehicle Batteries," in *IEEE Access*, vol. 8, pp. 155576-155589, 2020.
- [22] Y. Sun, H. Yue, J. Zhang and C. Booth, "Minimization of Residential Energy Cost Considering Energy Storage System and EV With Driving Usage Probabilities," in *IEEE Transactions on Sustainable Energy*, vol. 10, no. 4, pp. 1752-1763, Oct. 2019.
- [23] H. Farzin, M. Fotuhi-Firuzabad and M. Moeini-Aghaie, "A Practical Scheme to Involve Degradation Cost of Lithium-Ion Batteries in Vehicle-to-Grid Applications," in *IEEE Transactions on Sustainable Energy*, vol. 7, no. 4, pp. 1730-1738, Oct. 2016.
- [24] Z. Wei, Y. Li and L. Cai, "Electric Vehicle Charging Scheme for a Park-and-Charge System Considering Battery Degradation Costs," in *IEEE Transactions on Intelligent Vehicles*, vol. 3, no. 3, pp. 361-373, Sept. 2018.
- [25] S. Fang, B. Gou, Y. Wang, Y. Xu, C. Shang and H. Wang, "Optimal Hierarchical Management of Shipboard Multibattery Energy Storage System Using a Data-Driven Degradation Model," in *IEEE Transactions on Transportation Electrification*, vol. 5, no. 4, pp. 1306-1318, Dec. 2019.
- [26] P. Attia, M. Deetjen, and J. Witmer, "Accelerating battery development by early prediction of cell lifetime," (2018).
- [27] P. Attia, A. Grover, N. Jin et al., "Closed-loop optimization of fast-charging protocols for batteries with machine learning," in *Nature*, vol. 578, pp. 397–402, 2020.
- [28] K. Severson, P. Attia, N. Jin, et al., "Data-driven prediction of battery cycle life before capacity degradation," in *Nat Energy* vol. 4, pp 383–391, 2019.
- [29] Omar N., M. A. Monem, Y. Firouz, J. Salminen, J. Smekens, O. Hergazy, H. Gaulous, G. Mulder, P. Van den Bossche, T. Coosemans, and J. Van Mierlo, "Lithium iron phosphate based battery — Assessment of the aging parameters and development of cycle life model," *Applied Energy*, Vol. 113, January 2014, pp. 1575–1585.
- [30] S. Saxena, C. Floth, J. MacDonald. S. Moura, "Quantifying EV battery end-of-life through analysis of travel needs with vehicle powertrain models," in *Journal of Power Sources*, vol. 282, pp. 265-276. Jan. 2015.
- [31] S. Loffe, C. Szegedy, "Batch Normalization: Accelerating Deep Network Training by Reducing Internal Covariate Shift," in *Proceedings of the 32nd International Conference on Machine Learning*, Vol. 37, pp. 448-456, Mar. 2015.
- [32] NN-SVG, <http://alexlenail.me/NN-SVG/index.html>.
- [33] "Dataport Resources," May, 2019 [online] Available: <https://dataport.pecanstreet.org/academic>.
- [34] "ERCOT, Electric Reliability Council of Texas," [Online]. Available: <http://www.ercot.com/>.
- [35] "Pyomo, Python Software packages," Available: [Online]. Available: <http://www.pyomo.org/>.
- [36] "Gurobi Optimization, Linear Programming Solver," [Online]. Available: <https://www.gurobi.com/>.